applied sciences

MDPI

*Article*

# On the Performance of LDPC-Coded MIMO Schemes for Underwater Communications Using 5G-like Processing

**Mário Marques da Silva [1,2,3,*], Rui Dinis [1,3,4], José Aleixo [2,3] and Luís M. L. Oliveira [5]**

[1] Instituto de Telecomunicações, 1049-001 Lisboa, Portugal; rdinis@fct.unl.pt
[2] Department of Engeneering and Computer Sciences, Universidade Autónoma de Lisboa, 1169-023 Lisboa, Portugal; jaleixo@autonoma.pt
[3] Autonoma TechLab, 1169-023 Lisboa, Portugal
[4] Faculty of Sciences and Technology, Universidade Nova, 2829-516 Caparica, Portugal
[5] Centro de Investigação em Cidades Inteligentes, 2300-305 Tomar, Portugal; loliveira@ipt.pt
* Correspondence: mmsilva@autonoma.pt

**Abstract:** This article studies the underwater acoustic (UWA) communications associated with multiple input–multiple output (MIMO), single carrier with frequency-domain equalization (SC-FDE), and with low-density parity-check (LDPC) codes. Low-complexity receivers such as equal gain combining (EGC), maximum ratio combining (MRC), and iterative block—decision feedback equalization (IB-DFE) are studied in the above-described scenarios. Furthermore, due to the low carrier frequencies utilized in UWA communications, the performance of the proposed MIMO scenarios is studied at different levels of channel correlation between antennas. This article shows that the combined schemes tend to achieve good performances while presenting low complexity, even in scenarios with channel correlation between antennas.

**Keywords:** underwater communications; LDPC; MIMO; SC-FDE

**Citation:** Da Silva, M.M.; Dinis, R.; Aleixo, J.; Oliveira, L.M.L. On the Performance of LDPC-Coded MIMO Schemes for Underwater Communications Using 5G-like Processing. *Appl. Sci.* **2022**, *12*, 5549. https://doi.org/10.3390/app12115549

Academic Editors: Christos Bouras and Amalia Miliou

Received: 11 March 2022
Accepted: 28 May 2022
Published: 30 May 2022

**Publisher's Note:** MDPI stays neutral with regard to jurisdictional claims in published maps and institutional affiliations.



## 1. Introduction

Two-thirds of the Earth's surface corresponds to the sea, demanding connectivity in the new paradigm of the Fourth Industrial Revolution, namely, to interconnect Internet of Things (IoT) devices. Underwater acoustic (UWA) communications is the solution to solve this gap. However, due to the high level of multipath [1], impulsive noise, and low carrier frequencies, the bit rates available in UWA communications are low [2]. This limitation can be mitigated by employing techniques such as block transmission techniques, such as orthogonal frequency division multiplexing (OFDM) or single carrier with frequency-domain equalization (SC-FDE), as well as multiple input–multiple output (MIMO) systems, as adopted for the Fifth Generation of Cellular Communications (5G) [3].

MIMO systems bring added value in terms of capacity and diversity gains. However, such gains are conditioned on the existence of spatially uncorrelated channels. Due to the lower carrier frequencies employed in UWA scenarios, such condition is rarely fulfilled [4]. Since a certain level of channel correlation between signals of different antennas exists in real scenarios, such configuration is here considered.

The complexity of the UWA scenarios is defined by their non-homogeneity, being dependent on the following factors: pressure, temperature, and salinity. The propagation speed of the sound is affected by each of these factors [5]. Several expressions have been developed empirically to calculate sound propagation speed in UWA scenarios. Wilson defined in [5] the following expression widely utilized:

$$c = 1449 + 4.6T_C + 0.055T_C{}^2 + 0.003T_C{}^3 + (1.39 - 0.012T_C)(S - 35) + 0.17d_P \quad (1)$$

where $c$ stands for the propagation speed, $T_C$ the temperature in degrees Celsius, $S$ the salinity in parts per thousands, and $d_P$ the depth in meters.

Although there is complexity of propagation of sound in underwater scenarios, it is known that the increase of the number of antenna elements that comprise MIMO systems corresponds to a technique widely used to increase the capacity gains [6–8]. However, this demands higher signal processing levels associated with linear receivers, such as the zero forcing (ZF). Therefore, a solution to simplify the complexity relies on the use of sub-optimal receivers, such as equal gain combining (EGC), maximum ratio combining (MRC) [6,7], and iterative block—decision feedback equalization (IB-DFE), being studied in this article.

Low-density parity-check (LDPC) has been adopted by 3GPP as an encoding scheme for the 5G standard [9,10]. Before, LDPC codes were adopted for the long-term evolution (LTE), as well as for the World Interoperability for Microwave Access (WiMAX) standard. Due to its outstanding performance, LDPC codes have been utilized in other scenarios, such as in UWA communications.

Impulsive noise is typically experienced in low frequencies, consisting of short-duration noisy pulses (from a few microseconds up to milliseconds) [11–13]. This is caused by sea life activity in the underwater environment, which can be substantially above the additive white Gaussian noise (AWGN).

Previous works considered using the block transmission technique OFDM, in UWA communications, such as [14]. The work published in [11] focuses on impulsive noise superimposed on OFDM signals, including mitigation techniques. Furthermore, previous works have also considered the combination of OFDM, and MIMO systems applied to UWA communications [15,16]. Moreover, as compared to [17], the research published in this article considers LDPC codes and impulsive noise, which is typical of UWA communications. Moreover, channel estimation, using training sequences, is also adopted to make the results of this complex system more realistic.

This article studies the performance of UWA communications, using MIMO communication systems, for different levels of channel correlations between adjacent antenna elements of the MIMO configurations, with different receiver types, using LDPC codes, and using SC-FDE transmission. Instead of studying individual schemes, this article studies such a complex system, also considering impulsive noise, LDPC codes, and channel estimation.

This article is organized as follows: Section 2 describes the system and signal characterization, Section 3 analyses the performance results, and Section 4 concludes the article.

## 2. System and Signal Characterization

This article considers a multi-layer MIMO system, which requires a number of $R$ receiving antennas equal to or higher than $T$ transmitting antennas. It is considered that each transmitting antenna sends a different flow of symbols. On the other hand, the number of $R$ receiving antennas is responsible for providing diversity. SC-FDE signals are assumed [18], associated with quadrature phase shift keying (QPSK) modulation.

As depicted in Figure 1, the $n$th transmitted block, of $N$ data symbols, sent by the $t$th antenna is denoted as $x_n^{(t)}$, while the received block by the $r$th antenna is denoted as $y_n^{(r)}$. The mapping between the time domain signal and the frequency-domain signal for the transmitted block is defined as $DFT\{x_n^{(t)}; n = 0,1,...,N-1\} = \left\{X_k^{(t)}; k = 0,1,...,N-1\right\}$, i.e., by performing the discrete Fourier transform (DFT) of the time-domain block. Similar mapping is assumed for the received block as $DFT\{y_n^{(r)}; k = 0,1,...,N-1\} = \left\{Y_k^{(r)}; k = 0,1,...,N-1\right\}$

.

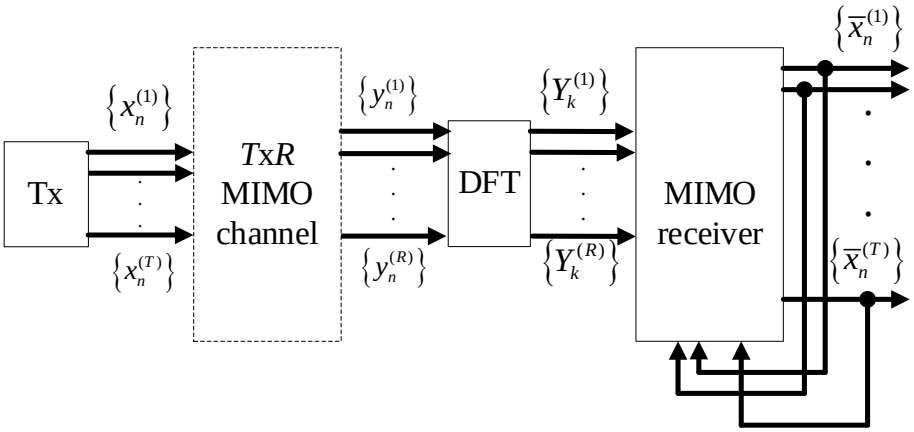


**Figure 1.** Block diagram of an m-MIMO system associated with SC-FDE signals.

After removing the cyclic prefix, and assuming a cyclic prefix longer than the overall channel impulse response of each channel, using the matrix-vector representation, the received frequency-domain signal comes:

$$\mathbf{Y}_k = \left[ Y_k^{(1)}, ..., Y_k^{(R)} \right]^T = \mathbf{H}_k \mathbf{X}_k + \mathbf{N}_k \quad (2)$$

where $\mathbf{X}_k = \left[ X_k^{(1)}, ..., X_k^{(T)} \right]^T$ stands for the frequency-domain transmitted data symbols, where $\mathbf{H}_k$ denotes the $R \times T$ channel matrix for the *k*th subcarrier, with $(r,t)$ th element $\mathbf{H}_k^{(t,r)}$, and where $H_k$ denotes the channel frequency response for the *k*th subcarrier (assumed invariant during the transmission of a given block). Note that the mapping between the channel time and frequency domains is defined by $\left\{ H_k ; k = 0,1,..., N-1 \right\} = DFT\left\{ h_n ; n = 0,1,..., N-1 \right\}$. Moreover, $N_k$ is the frequency-domain block channel noise for that subcarrier.

### *2.1. System and Signal Model for the Receivers*

A very efficient receiver commonly associated with SC-FDE schemes [18] is the IB-DFE. Such an iterative receiver uses feedforward and feedback coefficients to process the signals in the frequency domain, reaching a performance typically much better than that of a non-iterative receiver. IB-DFE can be viewed as turbo equalization [8,19].

The ZF receiver tends to be complex because it requires the computation of the pseudo-inverse of the channel matrix, for each frequency component. This article avoids this complexity by implementing the m-MIMO using MRC and EGC receivers, simplifying its processing. Furthermore, these receivers are iterative, being, in this study, associated with SC-FDE transmissions.

Assuming a non-iterative receiver, the estimated frequency-domain data symbols $\tilde{\mathbf{X}}_k = \left[ \tilde{X}_k^{(1)}, ..., \tilde{X}_k^{(R)} \right]^T$ comes:

$$\tilde{\mathbf{X}}_k = \mathbf{B}_k \mathbf{Y}_k \quad (3)$$

Depending on the algorithm, $\mathbf{B}_k$ can be computed as $\mathbf{B}_k = \mathbf{H}_k^H \left( \mathbf{H}_k \mathbf{H}_k^H \right)^{-1}$ for the ZF, as $\mathbf{B}_k = \mathbf{H}_k^H$ for the MRC, and as $\mathbf{B}_k = \exp\left\{ j \arg\left( \mathbf{H}_k^H \right) \right\}$ for the EGC [20].

As described, the ZF receiver is a linear algorithm that applies the pseudo-inverse of the channel's frequency response, for each frequency component of the channel. Therefore, the level of complexity and computation is very high, which also translates to high battery consumption. Moreover, the ZF is very efficient in removing the intersymbol interference but has the disadvantage of presenting noise enhancement when utilized in post-processing. Therefore, it tends to degrade the performance for average to high noise levels.

On the other hand, the MRC and EGC tend to mitigate these limitations due to their simplicity but generate some residual interference generated in the decoding process, especially for moderate values of $T/R$. This can be mitigated by employing an iterative receiver that implements the following function [20]:

$$\tilde{\mathbf{X}}_k = \mathbf{B}_k^H \mathbf{Y}_k - \mathbf{C}_k \bar{\mathbf{X}}_k, \tag{4}$$

where the interference cancelation matrix $\mathbf{C}_k$ can be computed as [20]:

$$\mathbf{C}_k = \mathbf{A}_k^H \mathbf{H}_k - \mathbf{I}, \tag{5}$$

and where $\mathbf{I}$ is an $R \times R$ identity matrix and where the $(i,i')$th elements of the matrix $\mathbf{A}$ are defined as $[\mathbf{A}]_{i,i'} = [\mathbf{H}]_{i,i'}^H$ for the MRC and $[\mathbf{A}]_{i,i'} = \exp\left(j \arg\left([\mathbf{H}]_{i,i'}\right)\right)$ for the EGC (i.e., they have absolute value 1 and phase identical to the corresponding element of the matrix $\mathbf{H}$).

### *2.2. Channel Estimation*

This article assumes that training sequences (pilots) are utilized to perform the channel estimation. The channel frequency response is defined as [21]:

$$\tilde{H}_k^{(t,r)} = \frac{Y_k^{(r)} X_k^{(t)TS*}}{2\sigma_{TS}^2} \tag{6}$$

where $X_k^{(t)TS}$ denotes the training sequence transmitted by the *t*th transmitting antenna $(t = 1, 2, .., T)$, $Y_k^{(r)}$ stands for the signal at the *r*th receiving antenna $(r = 1, 2, .., R)$ ($TS$ means training sequence), and $\sigma_{TS}^2$ stands for the power (variance) of the training sequences. In this estimation, it is assumed that that the training sequences associated with different transmitting antennas are orthogonal, leading to $X_k^{TS(m)} X_k^{TS(q)*} = 0 \quad m \neq q$. This leads to $\tilde{H}_k = H_k + \varepsilon_k$, where $\varepsilon_k$ stands for the channel estimation error, being Gaussian-distributed, with zero-mean, defined as

$$\mathrm{E}\left\{\left|\varepsilon_k\right|^2\right\} = \frac{\sigma_N^2}{\sigma_{TS}^2} \tag{7}$$

with $\sigma_N^2 = \mathrm{E}\left\{\left|N_k\right|^2\right\} \big/ 2$ and with $\sigma_{TS}^2 = \left|X_k^{TS}\right|^2 / 2$, as defined in [21].

In order to improve the channel estimates, the following enhancement can be employed [22,23]:

$$\widehat{H}_k^{(t,r)} = \mathrm{DFT}\left\{\tilde{h}_n^{(t,r)} w_n\right\}, \tag{8}$$

where $w_n = 1$ if the *n*th time-domain sample is inside the cyclic prefix, and 0 otherwise.

### *2.3. Impulsive Noise*

Impulsive noise [11–13] is typically experienced in low frequencies, consisting of short-duration noisy pulses. In the underwater environment, this is caused by sea life activity, which can be as high as 40 dB above the AWGN.

Impulsive noise can be acceptable in analog communications, being, however, disruptive in digital communications, originating a burst of errors. Therefore, the AWGN model is not well suited to model an environment characterized by impulsive noise. The Markov chain is an important model to characterize the impulsive noise, which is closer to the real environment [13]. The Markov chain is a model with memory because the next state depends on the actual state [13]. The Markov chain has four different models, known as binary state model, Markov–Middleton model, partitioned Markov chain, and second-level Markov chain [13]. As can be seen from Figure 2, the binary state model has two

states (0, 1), which best characterize the states of impulsive noise. The state $S_1$ represents the channel free of impulsive noise (good channel), while the $S_0$ represents the opposite (bad channel). The probability of transitions from $S_i$ to is given by the values $p_{i,j}$, $i, j \in \{0,1\}$ [13].

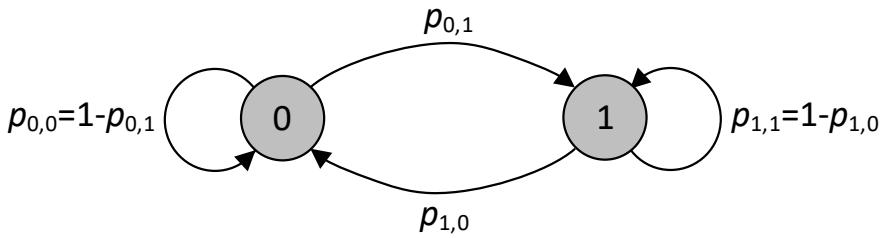


**Figure 2.** The Markov chain, binary state model [13].

### 3. Simulation Results and Analysis

The performance of the UWA communication, in terms of bit error rate (BER), is evaluated making use of Monte Carlo simulations, associated with SC-FDE block transmission technique and m-MIMO. The error probability, using BER as performance index, was evaluated as a function of $E_b / N_0$, where $E_b$ is the energy of the transmitted bits, and $N_0$ is the one-sided power spectral density of the noise. A block length of $N$ = 256 QPSK symbols was assumed. LDPC codes of length 32,400 were adopted, with a code rate of ½. This corresponds to 64,800 coded bits, whose sequence is generated as defined in [24]. A severe Rayleigh fading channel was considered with 20 uncorrelated equal power paths. This corresponds to a highly demanding channel, which can be viewed as a worst-case scenario for underwater propagation. The high number of multipaths and having all of them with the same average power makes this channel very destructive in terms of the creation of intersymbol interference, which can be viewed as the most disruptive cause that limits UWA communications. Channel estimation with training sequences is assumed. Multilayer MIMO is assumed (spatial multiplexing). Except for the ZF, the other receivers are iterative, canceling the residual interference generated in the decoding algorithm. Nevertheless, while the ZF is much more computationally demanding, the other receivers are not. We considered four iterations of the iterative receivers, as the performance improvement was almost negligible beyond four iterations. As defined in Section 2.3, the Markov chain, binary state model, was assumed to simulate the impulsive noise (in addition to other impairments, such as fading and AWGN noise), typically present in underwater scenarios. We considered $p_{1,0} = 0.1$ and $p_{0,1} = 0.8$. Moreover, we have defined the following probabilities: Prob(Good->Bad) = 0.1; Prob(Good->Good) = 0.9; Prob(Bad->Bad) = 0.2; Prob(Bad->Good) = 0.8, while in [11] a probability of $p_{1,0} = 0.0098$ was assumed (i.e., Prob(Good->Bad). Note that Prob(Good->Bad) stands for the probability of transition from Good to Bad state. Impulsive noise [11,12] may vary from symbol to symbol. Moreover, we assumed a variance of the impulsive noise (when in a bad state) 20 dB higher than the variance of AWGN noise. Table 1 presents a list of baseline simulations utilized in the different graphics of this section.

**Table 1.** List of baselines utilized in simulations.

| Figure | Diversity | Encoding | Channel Estimation | Channel Correlation | Impulsive Noise |
|---|---|---|---|---|---|
| Figure 3 | MIMO 4 × 32 | W/out LDPC | With ideal channel estimation | 0 | With and w/out |
| Figure 4 | MIMO 4 × 32 | With and w/out LDPC | With ideal channel estimation | 0 | With |
| Figure 5 | MIMO 4 × 32 | With LDPC | With channel estimation | 0 and 0.3 | With |
| Figure 6 | MIMO 4 × 32 | With and w/out LDPC | With channel estimation | 0.3 | With |
| Figure 7 | MIMO 4 × 32 | With LDPC | With channel estimation | 0.3, 0.5, and 0.7 | With |
| Figure 8 | MIMO 4 × 32 | With and w/out LDPC | With channel estimation | 0.5 | With |
| Figure 9 | MIMO 4 × 32 versus 4 × 256 | With LDPC | With channel estimation | 0.3 | With |

Figure 3 (baseline 1) shows the performance results for UWA communications with and without impulsive noise, with 4 × 32 MIMO, without LDPC codes, for four different receivers: the ZF, MRC, EGC, and IB-DFE. The matched filter bound (MFB) curve is a way to measure the channel modeled by the sum of delayed and independently Rayleigh-fading rays, which can be viewed as a lower bound. This graphic considers that the channel correlation between adjacent antenna elements of the MIMO system does not exist (correlation 0). Therefore, results with ideal channel estimation are considered in this graphic. As expected, the results obtained with impulsive noise are much worse than those only with AWGN noise for all the receivers. Nevertheless, it is known that the marine environment is characterized by the existence of impulsive noise generated by sea life activity, making this scenario more realistic.

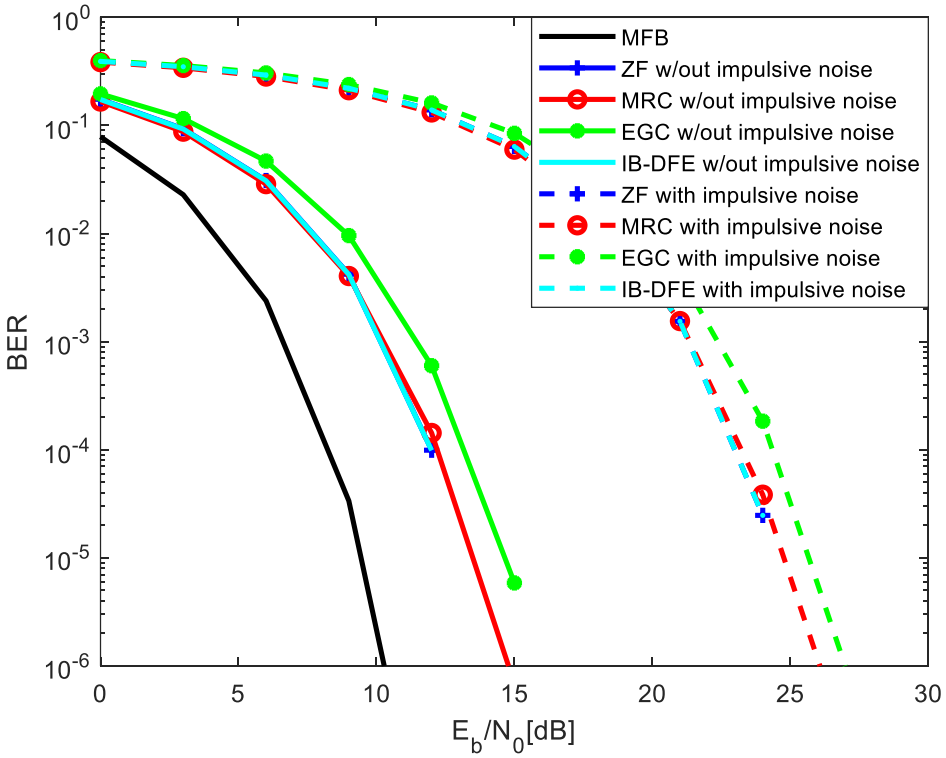


**Figure 3.** Results for 4 × 32 MIMO (with and without impulsive noise), without LDPC codes, with ideal channel estimation and without channel correlation between antennas.

When comparing the different receiver types, it is viewed that the MRC is the one that tends to achieve the best performance (while being less computational demanding than the ZF), while the EGC achieves the worst performance. The ZF and IB-DFE present the same results (these curves are superimposed, with and without impulsive noise). It is worth noting that such superposition of the IB-DFE over the ZF curves occurs in all graphics of this article. The Monte Carlo simulation considers the transmission of a high number sequence of bits, varying the noise and channel conditions in each sequence, and evaluating the number of corrupted bits. The BER is the quotient between the number of corrupted bits and the number of transmitted bits. The simulation time for this graphic was limited to approximately 6 h.

Figure 4 (baseline 2) shows the performance results for UWA communications with and without LDPC codes, with 4 × 32 MIMO, with impulsive noise, with ideal channel estimation, and without channel correlation between adjacent antenna elements. As expected, the use of LDPC codes corresponds to a performance improvement for all different receiver types. Furthermore, such performance improvement obtained with the LDPC codes is of the order of 5 dB. From these results, we can conclude that the LDPC codes, adopted for 5G communications, are also well suited for UWA communications. The simulation time using LDPC codes increases drastically, as compared to the uncoded scenario. This results from the fact that the required processing is higher and because the BER is lower. With a lower BER, the number of transmitted bits needs to be higher, such that the obtained BER can be viewed as an average value. The simulation time using LDPC codes was around 36 h.

Figure 5 (baseline 4) shows the performance results for UWA communications without channel correlation versus correlation 0.3 between adjacent antenna elements, for 4 × 32 MIMO, channel estimation, impulsive noise, and LDPC codes. As can be seen, having a channel correlation of 0.3 between antennas leads to a very low performance degradation relating to the configuration without correlation. Although of such low performance degradation, this configuration is more realistic because the UWA communications consider carrier frequencies of the order of 15 kHz, whose wavelength is too high. It is known that a minimum distance of around 3 to 4 wavelengths is required between adjacent antenna elements to assure uncorrelated signals, which is difficult to achieve in such a UWA scenario. As previously described, while the results without LDPC are of the order of 6 h, the simulation time using LDPC codes was around 32 h.

Figure 6 (baseline 5) shows the performance results for UWA communications with and without LDPC codes, with 4 × 32 MIMO, with impulsive noise, with ideal channel estimation, and with channel correlation 0.3 between adjacent antenna elements. Similar to the results without correlation (Figure 4), the use of LDPC codes corresponds to a performance improvement for all different receiver types, of the order of 5 dB. Nevertheless, above 25 dB, the MRC with LDPC codes degrade relating to the MRC without LDPC codes. The simulation time with channel correlation is the same as those without correlation (it varies manly with and without LDPC codes).

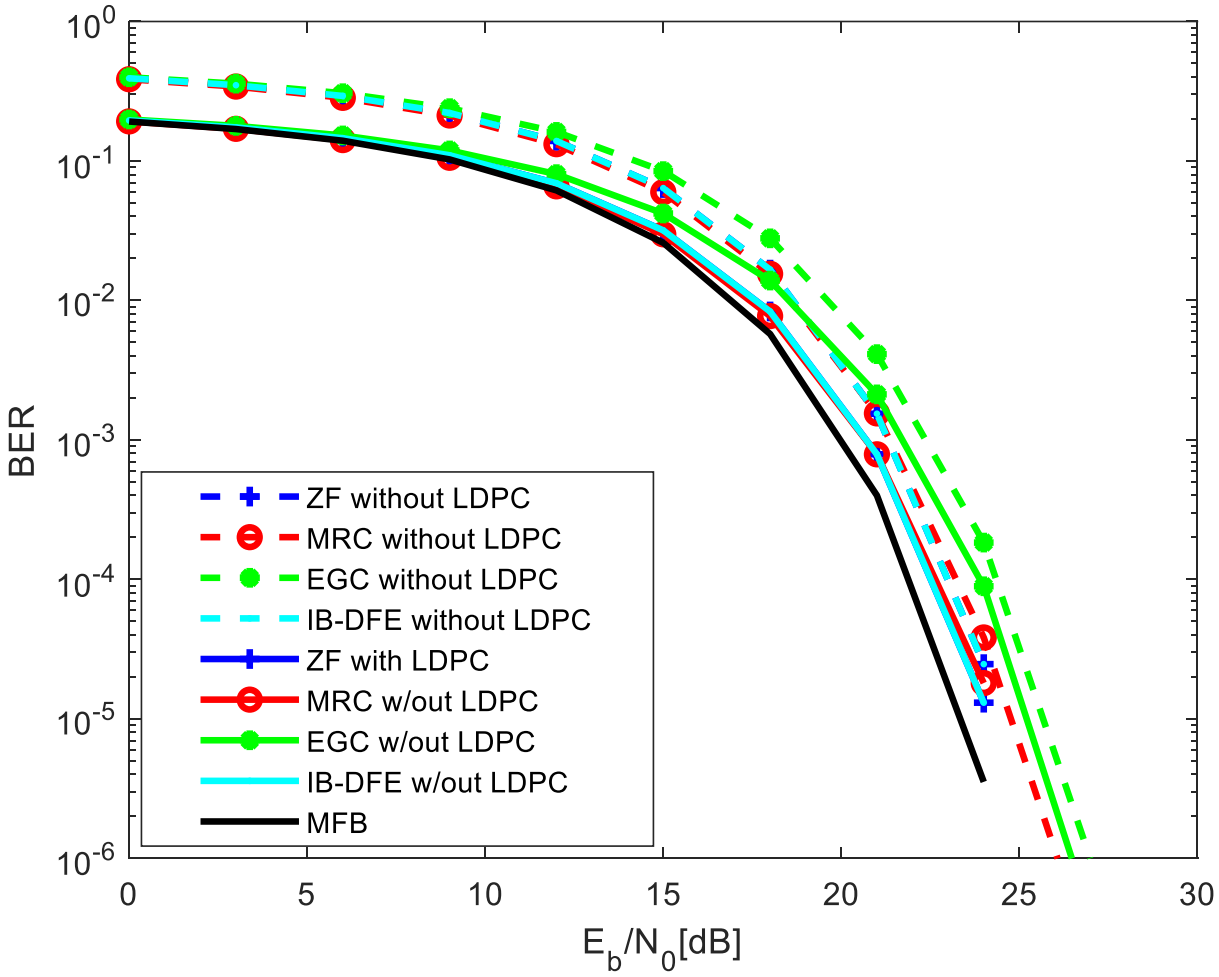


**Figure 4.** Results for 4 × 32 MIMO, with and without LDPC codes, with impulsive noise, with ideal channel estimation and without channel correlation between antennas.

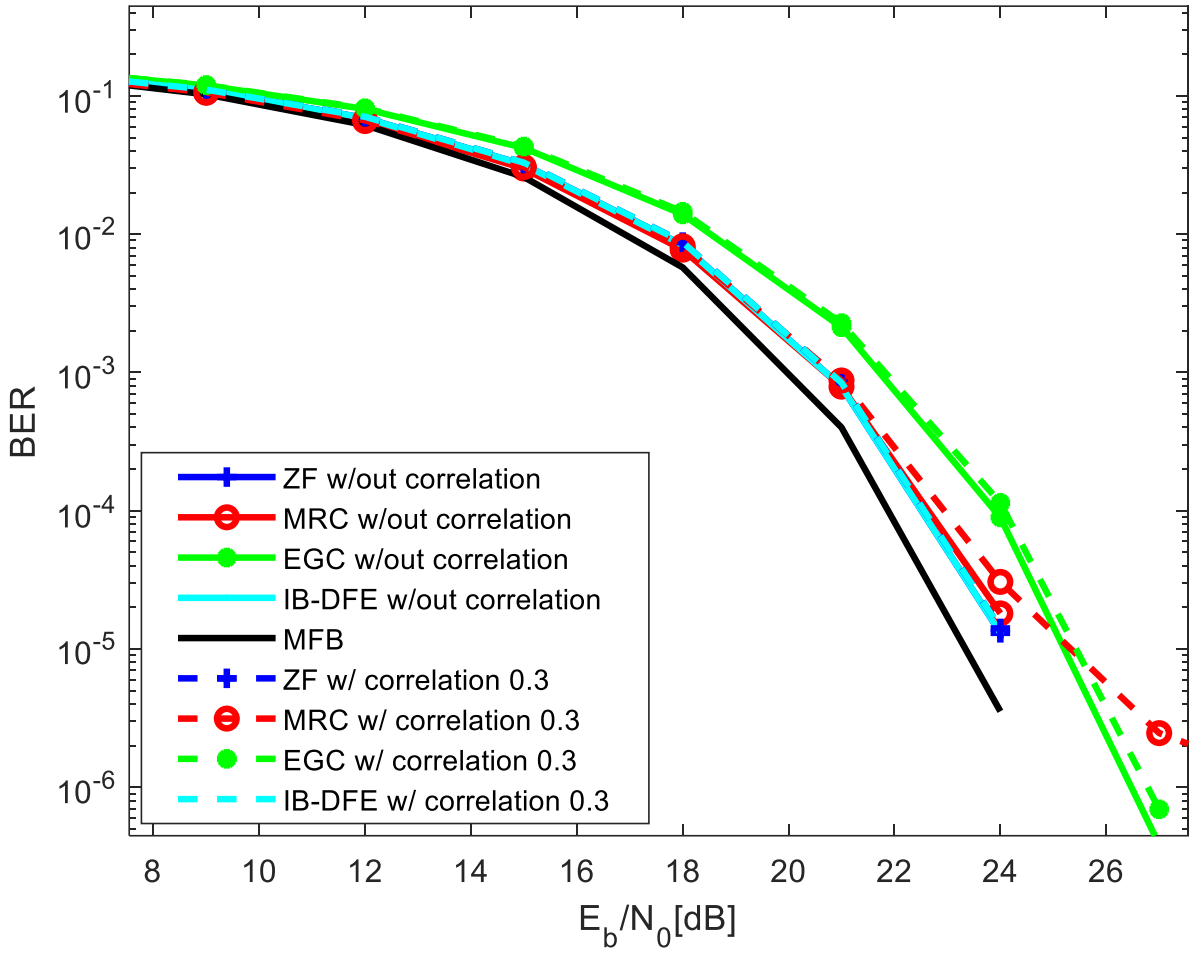


**Figure 5.** Results for 4 × 32 MIMO, with channel estimation, with impulsive noise, with LDPC codes, and without channel correlation versus with correlation 0.3 between antenna elements.

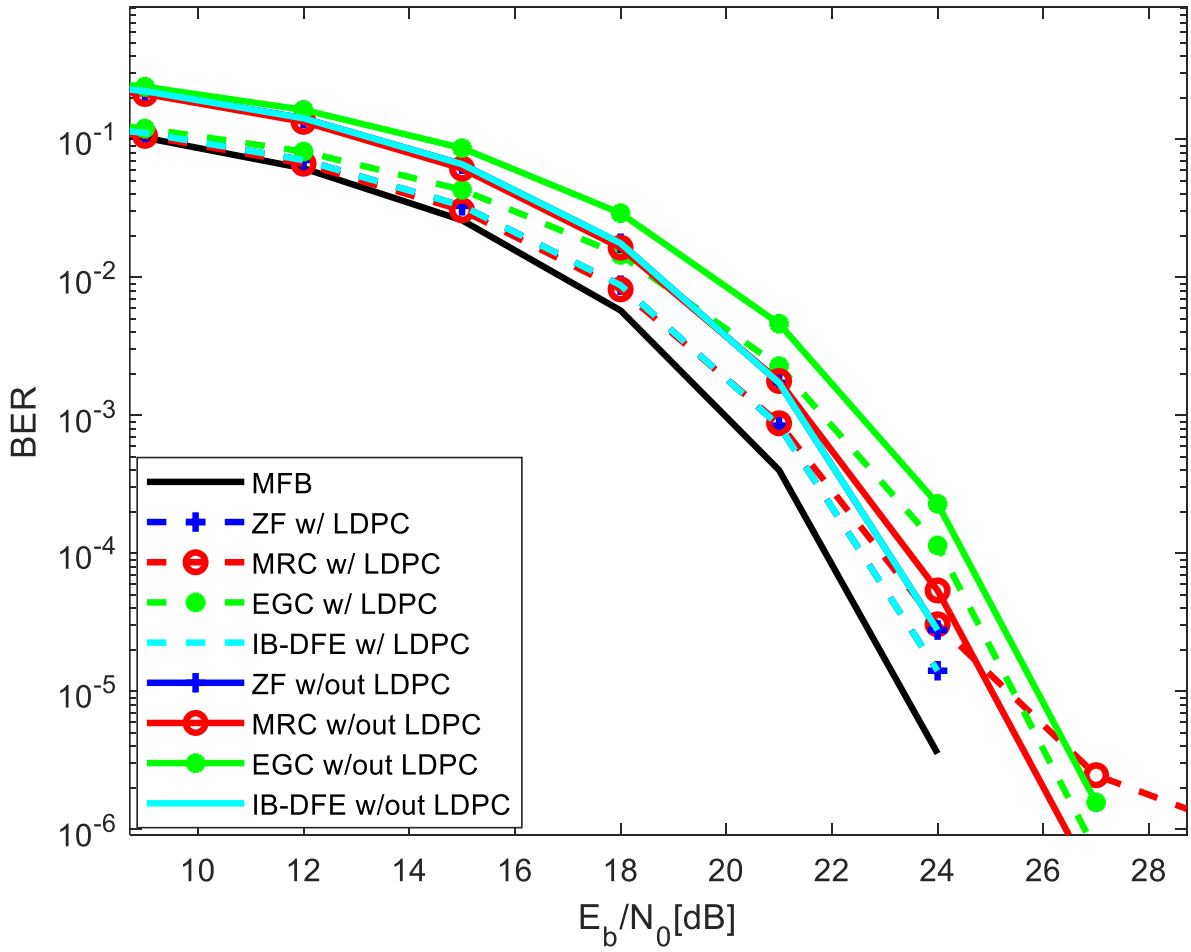


**Figure 6.** Results for 4 × 32 MIMO, with and without LDPC codes, with impulsive noise, with channel estimation, and with channel correlation 0.3 between antenna elements.

Figure 7 (baseline 6) shows the performance results for UWA communications with channel correlation 0.3 versus 0.5 and 0.7 between adjacent antenna elements, for 4 × 32 MIMO, channel estimation (pilots), impulsive noise, and LDPC codes. As expected, increasing the level of channel correlation leads to a performance degradation. Moreover, the performance degradation observed when we switch from correlation 0.3 into 0.5 is moderate. Nevertheless, such performance degradation increases drastically when we switch from correlation 0.5 into 0.7, especially for the MRC and EGC. It is viewed that the MRC and EGC receivers degrade heavily when we increase the channel correlation. It is worth noting that the channel correlation is a result of a reduced separation between antenna elements. An uncorrelated channel requires a typical separation of 3 to 5 wavelengths. In UWA communications, where carrier frequencies of the order of 15 kHz are employed, such separation is difficult to achieve. Therefore, studying the performance with different values of channel correlation is important to evaluate the different receivers. Naturally, the channel correlation depends on the carrier frequency and distance, making it worth studying the performance as a function of different channel correlation values, rather than of the distance.

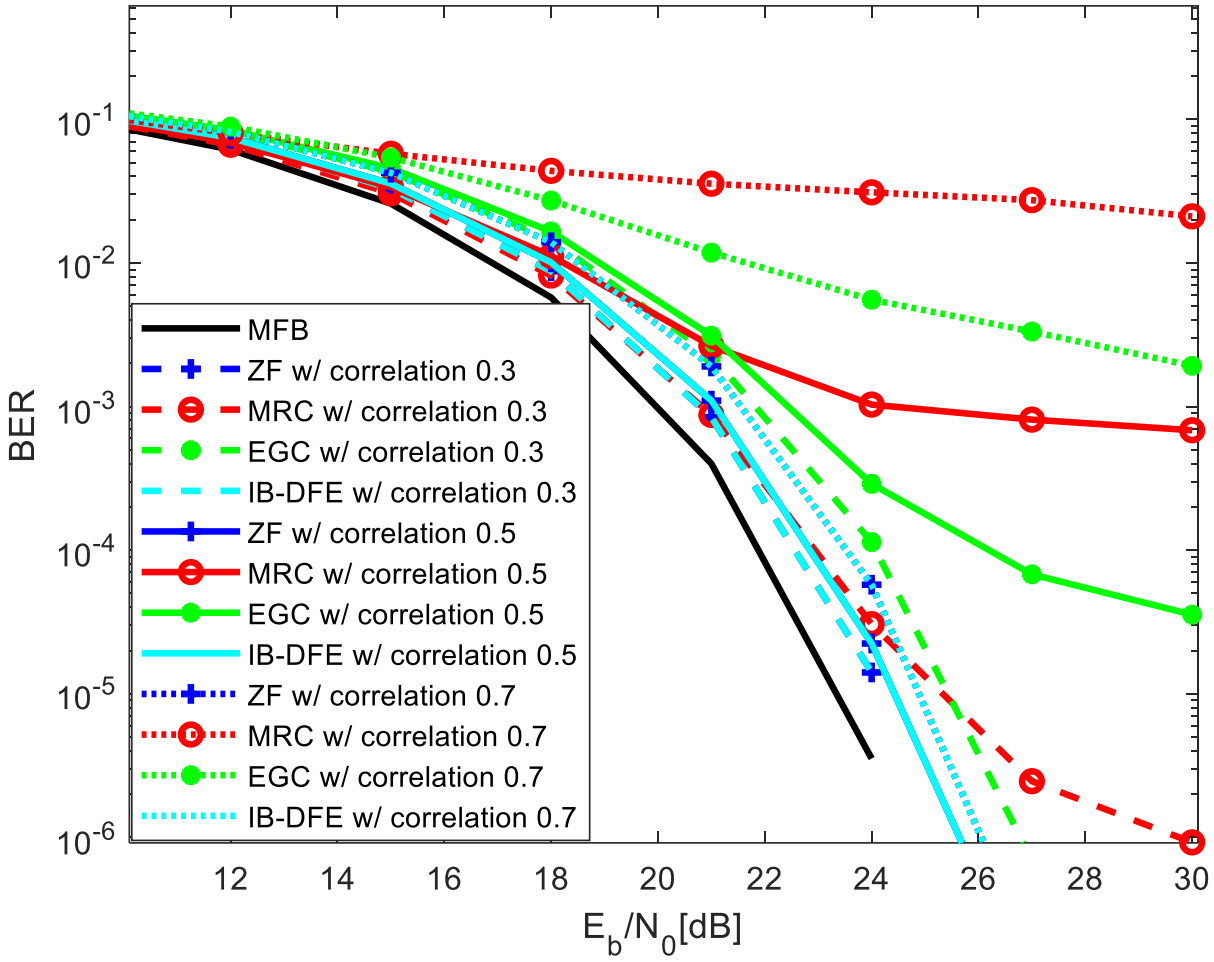


**Figure 7.** Results for 4 × 32 MIMO, with channel estimation, impulsive noise, LDPC codes, and channel correlation 0.3 versus 0.5 and 0.7 between antenna elements.

Figure 8 (baseline 7) shows the performance results for UWA communications with and without LDPC codes, with 4 × 32 MIMO, impulsive noise, ideal channel estimation, and channel correlation 0.5 between adjacent antenna elements. Similar to results without correlation (Figure 4) and results with correlation 0.3 (Figure 6), the use of LDPC codes corresponds to a performance improvement for all different receiver types, except above 25 dB and for the MRC and EGC receivers. The performance improvement obtained with LDPC codes is of the order of 5 dB.

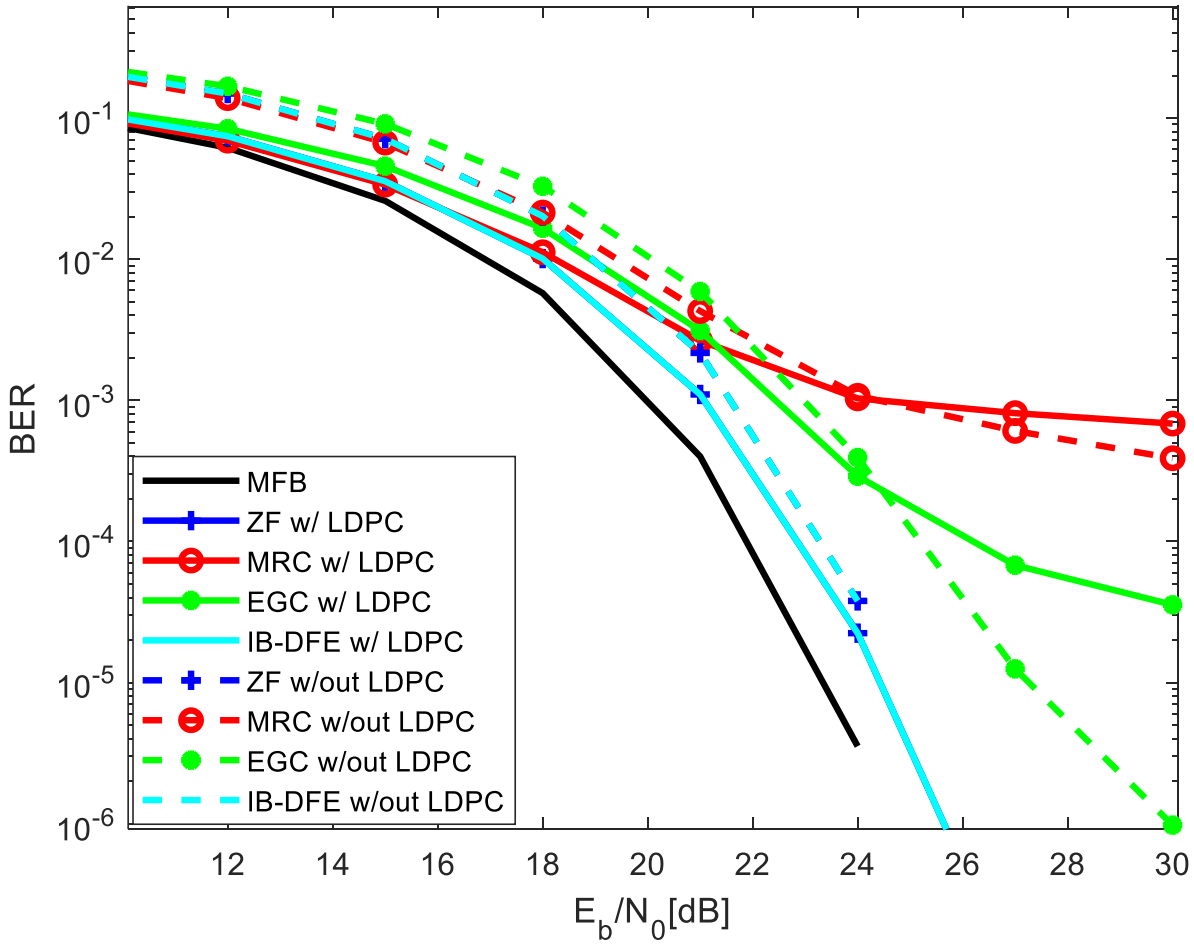


**Figure 8.** Results for 4 × 32 MIMO, with and without LDPC codes, impulsive noise, channel estimation, and channel correlation 0.5 between antenna elements.

Figure 9 (baseline 8) shows the performance results for UWA communications with 4 × 32 versus 4 × 256 MIMO, LDPC codes, impulsive noise, ideal channel estimation, and channel correlation 0.3 between adjacent antenna elements. Since MIMO multi-layer transmission was employed (spatial multiplexing), the number of transmitting antennas corresponds to the number of parallel flows of data, while the number of receiving antennas provides diversity. Therefore, 4 × 256 MIMO has a diversity eight times higher than 4 × 32. This translates into an improvement of performance for all receiver types. In the scenario of 4 × 32 MIMO, we observe that the MRC performance tends to degrade above 25 dB, while the ZF and IB-DFE performances are very close to the MFB. Nevertheless, with 4 × 256 MIMO, the MRC performs very close to the MFB and similar to the ZF and IB-DFE (these curves are almost superimposed). This occurs because the level of residual interference mitigated by the iterative receiver of the MRC is more accurately estimated and canceled due to the higher level of diversity provided by the 4 × 256 MIMO. The simulation time of 4 × 256 MIMO and LDPC codes is around 48 h, while 4 × 32 MIMO and LDPC codes it corresponds to around 36 h.

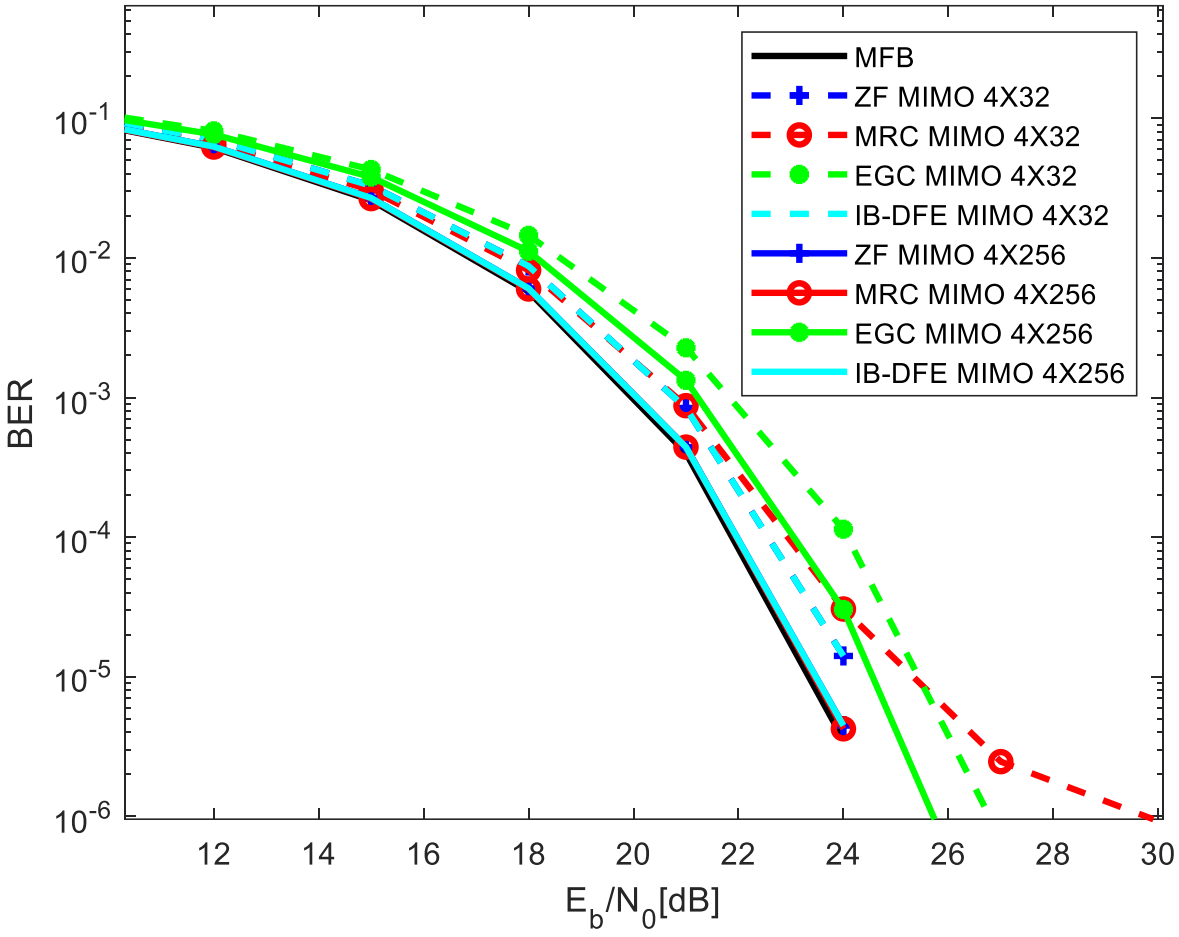


**Figure 9.** Results for 4 × 32 MIMO versus 4 × 256 MIMO, LDPC codes, impulsive noise, channel estimation, and channel correlation 0.3 between antenna elements.

## 4. Conclusions

This article publishes the results of a study of LDPC-coded UWA communications, with m-MIMO and SC-FDE transmission technique, for four different receiver types: ZF, MRC, EGC, and IB-DFE. It was viewed that the IB-DFE tends to achieve the best overall performance, while the level of computational demand is highly reduced as compared to ZF, which also translates into less battery consumption. It was also viewed that a channel correlation of 0.3 or 0.5 between adjacent antenna elements could still be accepted because their performance degradation, as compared with the scenario without channel correlation, is moderate. Regardless of such performance degradation, this configuration is more realistic because the UWA communications consider carrier frequencies of the order of 15 kHz, whose wavelengths are too high. It is known that a minimum distance of around 3 to 4 wavelengths is required between adjacent antenna elements to ensure uncorrelated signals, which is difficult to achieve in such a UWA scenario. It was also viewed that increasing the correlation between adjacent antenna elements to 0.7 makes the system almost unacceptable, as it heavily degrades the performance.

It was shown that increasing the number of receiving antennas of the MIMO system leads to a more accurate estimation and cancelation of the residual interference of the iterative receivers (MRC and IB-DFE), improving their performances closer to the MFB. This occurs because this article considers spatial multiplexing MIMO (multi-layer transmission), where the number of receiving antennas corresponds to the diversity order.

Finally, it can be concluded that for the UWA environment, a system composed of LDPC codes associated with m-MIMO, using SC-FDE signals, and with the low complexity reached with the MRC receiver, makes such a composed system a good combination to achieve future evolutions of UWA communications, even in the presence of impulsive noise.

**Author Contributions:** Conceptualization, M.M.d.S., R.D., J.A. and L.M.L.O. All authors have read and agreed to the published version of the manuscript.

**Funding:** This work is funded by FCT/MCTES through national funds and when applicable co-funded EU funds under the project UIDB/EEA/50008/2020.

**Informed Consent Statement:** Not applicable.

**Data Availability Statement:** Data was obtained through Monte Carlo Simulations, using Matlab, implemented by the authors.

**Acknowledgments:** We acknowledge the support of FCT/MCTES, as described above in Funding. We also acknowledge the support of Autonoma TechLab for providing an interesting environment to carry out this research.

**Conflicts of Interest:** The authors declare no conflict of interest.

## References

1. Stojanovic, M.; Preisig, J. Underwater acoustic communication channels: Propagation models and statistical characterization. *IEEE Commun. Mag.* **2009**, *47*, 84–89.
2. Zhou, S.; Wang, Z. *OFDM for Underwater Acoustic Communications*; Willey: Des Moines, IA, USA, 2016; pp. 76–103.
3. da Silva, M.M.; Dinis, R.; Martins, G. On the Performance of LDPC-Coded Massive MIMO Schemes with Power-Ordered NOMA Techniques. *Appl. Sci.* **2021**, 11, 8684. https://doi.org/10.3390/app11188684.
4. Xu, L.; Xu, T. *Digital Underwater Acoustic Communications*, 1st ed.; Academic Press: New York, NY, USA, 2016; pp. 55–78.
5. United States Naval Academy. Principles of Underwater Sound. Fundamentals of Naval Weapons Systems. Available online: https://man.fas.org/dod-101/navy/docs/fun/part08.htm (accessed on 15 November 2021).
6. Montezuma, P.; Borges, D.; Dinis, R. *Low Complexity MRC and EGC Based Receivers for SC-FDE Modulations with Massive MIMO Schemes*; IEEE GLOBALSIP: Washington, DC, USA, 2016.
7. da Silva, M.M.; Dinis, R. A simplified massive MIMO implemented with pre or post-processing. *Phys. Commun.* **2017**, *25*, 355–362. https://doi.org/10.1016/j.phycom.2017.06.002.
8. da Silva, M.M.; Monteiro, F.A. *MIMO Processing for 4G and beyond: Fundamentals and Evolution*; CRC Press Auerbach Publications: Boca Raton, FL, USA, 2014; ISBN 9781466598072. Available online: http://www.crcpress.com/product/isbn/9781466598072 (accessed on 15 November 2021).
9. Xu, J.; Xu, J. Structured LDPC Applied in IMT-Advanced System. In Proceedings of the International Conference on Wireless Communications Networking & Mobile Computing, Dalian, China, 12–17 October 2008; pp. 1–4.
10. Li, L.; Xu, J.; Xu, J.; Hu, L. LDPC design for 5G NR URLLC & mMTC. In Proceedings of the 2020 International Wireless Communications and Mobile Computing (IWCMC), Limassol, Cyprus, 15–19 June 2020; pp. 1071–1076. https://doi.org/10.1109/IWCMC48107.2020.9148187.
11. Zhou, Y.; Yang, X.; Tong, F. Impulsive noise and carrier frequency offset cancellation for underwater acoustic OFDM communications. In Proceedings of the WUWNet'21: The 15th International Conference on Underwater Networks & Systems, Shenzhen, China, 22–24 November 2021; pp. 1–5. https://doi.org/10.1145/3491315.3491325.
12. Barazideh, R.; Sun, W.; Natarajan, B.; Nikitin, A.V.; Wang, Z. Impulsive noise mitigation in underwater acoustic communication systems: experimental studies. In Proceedings of the 2019 IEEE 9th Annual Computing and Communication Workshop and Conference (CCWC), Las Vegas, NV, USA, 7–9 January 2019.
13. Torres Gómez, J. A Survey on Impulsive Noise Modeling. *Rev. Telemática* **2017**, *16*, 101–113.
14. Cheng, X.; Yang, L.; Cheng, X. *Cooperative OFDM Underwater Acoustic Communications*; Springer: New York, NY, USA, 2016; pp. 34–54.
15. Li, B.; Huang, J.; Zhou, S.; Ball, K.; Stojanovic, M.; Freitag, L.; Willett, P. MIMO-OFDM for High-Rate Underwater Acoustic Communications. *IEEE J. Ocean. Eng.* **2009**, *34*, 634–644.
16. Qiao, G.; Babar, Z.; Ma, L.; Liu, S.; Wu, J. MIMO-OFDM underwater acoustic communication systems—A review. *Phys. Commun.* **2017**, *23*, 56–64.
17. Da Silva, M.M.; Aleixo, J.; Guerreiro, J.; Dinis, R.; Montezuma Carvalho, P. Performance Evaluation of Low-complexity Receivers for MIMO Underwater Spatially Correlated Channels. In Proceedings of the 41st Progress in Electromagnetics Research Symposium 2017 (PIERS 2019), Rome, Italy, 17–20 June 2019.

18. Benvenuto, N.; Dinis, R.; Falconer, D.; Tomasin, S. Single Carrier Modulation with Non-Linear Frequency Domain Equalization: An Idea Whose Time Has Come—Again. *IEEE Proc.* **2010**, *98*, 69–96.
19. Tuchler, M.; Koetter, R.; Singer, A. Turbo equalization: principles and new results. *IEEE Trans. Commun.* **2002**, *50*, 754–767.
20. Da Silva, M.M.; Dinis, R.; Guerreiro, J. A Low Complexity Channel Estimation and Detection for Massive MIMO Using SC-FDE. *Telecom* **2020**, *1*, 3–17. Available online: https://www.mdpi.com/2673-4001/1/1/2/htm (accessed on 21 November 2021).
21. Da Silva, M.M.; Dinis, R.; Guerreiro, J. Implicit Pilots for an Efficient Channel Estimation in Simplified Massive MIMO Schemes with Precoding. *Int. J. Antennas Propag.* **2019**. https://doi.org/10.1155/2019/5051963. Available online: https://www.hindawi.com/journals/ijap/2019/5051963/ (accessed on 15 November 2021).
22. van de Beek, J.; Edfors, O.; Sandell, M.; Wilson, S.K.; Borjesson, P.O. On Channel Estimation in OFDM Systems. In Proceedings of the IEEE Vehicular Technology Conference 1995 (VTC'95), Chicago, IL, USA, 26–28 July 1995.
23. Edfors, O.; Sandell, M.; van de Beek, J.; Wilson, S.K.; Börjesson, P.O. Analysis of DFT-Based Channel Estimators for OFDM. *Wirel. Pers. Commun.* **2000**, *12*, 55–70.
24. Sarah, J. Introducing Low-Density Parity-Check Codes. 2010. Available online: http://citeseerx.ist.psu.edu/viewdoc/summary?doi=10.1.1.165.258 (accessed on 11 March 2022).